Catalysis Today 172 (2011) 48–52

Contents lists available at ScienceDirect

Catalysis Today

journal homepage: www.elsevier.com/locate/cattod

Novel nanohybrid materials based on L-leucine on hydrotalcite clays: Asymmetric epoxidation reaction of chalcona

Ronald-Alexander Miranda[a], Jordi Llorca[b,c], Elisabetta Finocchio[d], Gianguido Ramis[d], Francisco Medina[a], Jesús E. Sueiras[a], Anna M. Segarra[a,*]

[a] Departament d'Enginyeria Química, Universitat Rovira I Virgili Av. Països Catalans, 26, Campus Sescelades, Tarragona 43007, Spain
[b] Institut de Tècniques Energètique, Universitat Politècnica de Catalunya Diagonal 647, ed. ETSEIB, Barcelona 08028,Spain
[c] Centre for Research in NanoEngineering (CRnE-UPC), Universitat Politècnica de Catalunya, Pasqual i Vila 1-15, 08028 Barcelona, Spain
[d] Dipartimento di Ingegneria Chimica e di Processo, University of Genova, P.le Kennedy 1, 16129 Genova, Italy

ARTICLE INFO

Article history:
Received 1 December 2010
Received in revised form 7 February 2011
Accepted 14 February 2011
Available online 6 May 2011

Keywords:
Hydrotalcites
Nanohybrids materials
Julià–Colonna reaction
Asymmetric catalysis
Chalcona
Epoxidation

ABSTRACT

The assembly of biorgano-guest to laminar inorganic solids is of increasing interest to their versatile applications in biotechnology or catalysis. We synthesized two different biohybrid materials based on L-leu into the hydrotalcite rehydrated under ultrasound treatment (HT_{rus}), in which L-leu was immobilized by intercalation or by replacing of hydroxyl ions at the edge sites of HT_{rus}. Separately L-leu and HT_{rus} as catalysts showed very poor activity and lack of enantioselectivity in the epoxidation reaction of α,β-unsaturated ketones such as chalcone. Nevertheless, the catalysts presented high activity and even enantioselectivity towards the *trans*-(R,S)-epoxide depending on the L-leu location on the nanohybrid catalyst.

1. Introduction

Biohybrid nanostructured materials based on the combination of laminar inorganic solids such as hydrotalcites (HTs) and naturally occurring organo-molecules such as the amino acids (AAs) have received considerable attention due to their importance in catalysis, regenerative medicine, nanocomposite materials engineering etc. [1–3]. In addition, they find industrial interest since they are derived from abundant, cheap, and ecological sources. The biohybrid materials not only often exhibit highly complementary properties between their assembled components but also present new and interesting properties due to a synergistic effect [4–8]. These new and easily recovered materials may represent a big breakthrough in the pharmaceutical industry as they could replace current homogeneous catalysts which are difficult to separate and reuse. Particularly, hydrotalcite-like compound are widely used in the synthesis of bio-nanohybrids materials [2,9–15] because they possess suitable characteristics such as high surface area, swelling properties, high ion-exchange capacity and catalytic activity in several reactions. HTs are well known as anionic clay and layered double hydroxide compounds. The chemical composition of the HTs is $M_{1-x}{}^{2+}M_x{}^{3+}(OH)_2(A^{n-})_{x/n}.yH_2O$. The hydrotalcite-like compound structure consists of brucite-like layers $[Mg(OH)_2]$ with edge-sharing hydroxyl octahedral occupied by bivalent (Mg^{2+}) and trivalent (Al^{3+}) cations. The positive charged of the layers is balanced by anions located in the interlayer which can be exchanged by other organic or inorganic anions [16]. These materials can reconstruct the original layered structure after being calcined by rehydration in a CO_2 free atmosphere. The rehydrated hydrotalcite also called meixnerite, contains interlayer OH^- anions which provide significant Brønsted basic properties [17,18].

The negatively charged AAs (formed in basic medium) are potential chiral biocatalysts suitable for being immobilized in layered double hydroxides compounds such as HTs. Different methodologies for immobilising AAs into HTs have been developed. The L-pro/HT biohybrid synthesized by co-precipitation method was used as asymmetric catalyst in C–C bond-forming reactions [15]. The authors suggested that the L-pro was mainly located at the edges of the hydrotalcite layers. The biohybrid catalyst resulted in a higher catalytic activity than pure L-pro, although asymmetric induction was lower. Hibino also used the co-precipitation method immobilising the AAs between the hydrotalcite layers [19]. Later, Pitchumani et al. also interspersed the L-pro but by ion-exchange [2]. This biohybrid catalyst improved the enantioselectivity of

---

[*] Corresponding author. Tel.: +34 977 559651; fax: +34 977 559621.
E-mail address: anamaria.segarra@urv.cat (A.M. Segarra).

0920-5861/$ – see front matter © 2011 Elsevier B.V. All rights reserved.
doi:10.1016/j.cattod.2011.02.040

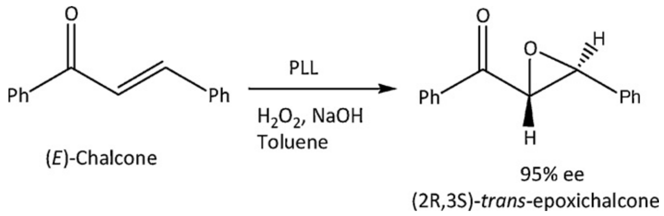

Scheme 1. Julia–Colonna asymmetric epoxidation of chalcone.

the not-immobilized L-pro in the Michael addition reaction of nitroalkenes with ketones. Furthermore, in some cases, the heterogenized catalyst presented an inversion in enantioselectivity compared to pure L-pro catalyst. To the best of our knowledge, all the reported protocols for synthesising AA-HT biohybrids require long time (>12 h).

Recently, our group has developed new protocols for synthesising nanolaminar hydrotalcite compounds using ultrasound treatment (HT_{rus}) which can incorporate highly efficient catalytic sites in the interlaminar space [20]. The properties of these HT_{rus} compounds make them a very attractive host structure for chiral molecules such as AAs which are able to catalyze the production of important chiral drugs. Several drugs such as Taxol (cancer chemotherapy) [21], (+)-Clausenamide (antiamnaesic agent) [22], Statin (cholesterol-lowering drug)[23] or (+)-Fenoprofen (rheumatoid arthritis) [24] are synthesized from chiral epoxide obtained by asymmetric epoxidation of α,β-unsaturated ketones. This reaction, known as Julià–Colonna, is catalyzed by the poly-L-leu (PLL) (Scheme 1) [25,26]. The PLL is synthesized by several steps and recovered after the reaction with difficulty.

Although the Julià–Colonna epoxidation mechanism is not at all clear, experiment and molecular modelling suggest that the helicity of the PLL determines the epoxide configuration through face-selective delivery of a hydroperoxide anion. Five L-leu residues were found to be sufficient to catalyze the Julià–Colonna epoxidation of chalcone with 96–98% ee [27]. In addition, the COOH-terminal group of the PLL does not seem to participate in the catalytic process.

Taking all this into consideration, we explored the possibility of developing new efficient synthetic protocols of different L-leu/HT_{rus} compounds where the combination of the layered materials and intercalation techniques offer new hybrid materials with desired properties. For first time, the L-leu/HT_{rus} biohybrids is used as catalysts in asymmetric Julià–Colonna epoxidation reaction, achieving higher activity and selectivity in the catalytic reaction of interest like the PLL.

2. Experimental

2.1. Synthesis of nanohybrid materials

2.1.1. Synthesis of rehydrated hydrotalcite (HT_{rus})

Mg–Al hydrotalcite (HT) with Mg/Al molar ratio = 2:1 containing nitrates as compensation anion was synthesized by the co-precipitation method at constant pH 10 [28]. Then, the HT was decomposed by thermal treatment at 450 °C during 15 h in air atmosphere and rehydrated in decarbonated water under ultrasound treatment according to the Medina et al. protocol [20]. Total rehydration of the HT was confirmed by ^{27}Al Magic-angle-spin (MAS) NMR. The obtained solid was denoted as HT_{rus}.

2.1.2. Synthesis of nanohybrid material

Nanohybrids were obtained using 20 ml of a solution of L-leu in decarbonated water at certain concentrations and HT_{rus} (500 mg). The immobilized process was performed employing two different methods. In the immobilization process by method A, the mixture was stirred for 30 min at room temperature under argon atmosphere. After immobilization process the obtained materials were separated by filtration, washed several times with decarbonated water and dried under argon. The variation in the concentration of the L-leu solution was performed to obtain different kind of materials which were denoted as L-leu/HT_{rus}-A_x, where x is the mmol of L-leu per mmol of Al^{3+} and correspond to 0.08, 0.22 and 0.44. In the immobilization process by method B, the mixture was stirred for 3 h at 80 °C under argon atmosphere. After immobilization process the obtained materials were separated by filtration, washed several times with decarbonated water and dried under argon. The nanohybrid material obtained was denoted as L-leu/HT_{rus}-$B_{1.09}$.

2.2. Characterization

The amount of L-leu immobilized onto HT_{rus} was determinate on a Shimatzu TOC-5000A in the combustion method at 953 K. Determination of the structural properties, material morphology and intercalation behaviour of the L-leu onto the HT layers were confirmed by powder XRD, FT-IR, ^{13}C and ^{27}Al MAS NMR and High-Resolution Transmission Electron Microscopy (HRTEM). Powder XRD measurements were performed on a Bruker-AXS D8-Discover diffractometer with 2θ angle ranging from 1° to 70°. FTIR spectra were recorded on a Nicolet Nexus Fourier Transform instrument provided with a DTGS KBr detector: for each spectrum 100 scans in the range 4000–400 cm^{-1} were recorded, resolution 4 cm^{-1}. HRTEM were performed with a JEOL 2010F instrument working at an acceleration voltage of 200 kV and equipped with a field emission source. The point-to-point resolution of the microscope was 0.19 nm and the resolution between lines was 0.14 nm. ^{13}C and ^{27}Al MAS-NMR spectra were obtained on a Varian Mercury VXR-400S spectrometer operating at 104.2 MHz with a pulse width of 1 ms. A total of 4000 scans were collected with a sweep width of 100 kHz and an acquisition time of 0.2 s. An acquisition delay of 1 s between successive accumulations was selected to avoid saturation effects.

2.3. Asymmetric Julià–Colonna epoxidation reaction

The asymmetric epoxidation reaction was performed in a tube of 10 ml where synthesized nanohybrid catalyst containing 0.44 mmol of L-leu (which corresponds to 458, 199, 125 and 80 mg of L-leu/HT_{rus}-$A_{0.08}$, L-leu/HT_{rus}-$A_{0.22}$, L-leu/HT_{rus}-$A_{0.44}$ and L-leu/HT_{rus}-$B_{1.09}$, respectively) tetrabutylammonium bromide (0.042 mmol), NaOH 5 M (0.43 ml) and hexane (3 ml) were mixed. Subsequently $H_2O_{2(aq)}$ (0.19 ml) and chalcone (1.44 mmol) were added. The mixture was stirred for 90 min at room temperature. To work-up the mixture, it was diluted in 1 ml of ethylacetate. The catalyst (solid phase) was washed several times with hexane and separated by centrifugation. The organic fraction was dried with $MgSO_4$. Then, the solvent in the organic phase was evaporated. The product was identified by ^{1}H NMR (400 MHz, $CDCl_3$): δ = 4.01 (s, 1H), 4.23 (s,1H), 7.32–7.45 (m,7H), 7.54 (d, 1H), 7.94 (d, 2H) ppm. The ee of *trans*-(2R,3S)-epoxy-1,3-diphenyl-propan-1-one formed by L-leu/HT catalyst was determinated by chiral HPLC using a ChiralPak IA column. The mobile phase was 25% hexane in ethanol, at a flow rate of 1 ml/min. The wavelength reading was 254 nm. The retention times were t_{major} = 7.6 min and t_{minor} = 10.6 min.

3. Results and discussion

3.1. Characterization results

In the present study, the immobilized amount of L-leu and the location of the AAs in the HT_{rus} were precisely controlled by changing the concentration of L-leu solution, the temperature and

Table 1
Composition and characteristics of the L-leu/HT$_{\text{rus}}$ nanohybrids synthesized.

Entry	Nanohybrid	L-leu amount immobilized (mmol L-leu/mmol Al^{3+}) [c]	d_{003} (Å)
1	HT$_{\text{rus}}$	–	7.7
2	L-leu/HT$_{\text{rus}}$-A$_{0.08}$ [a]	0.08	7.7
3	L-leu/HT$_{\text{rus}}$-A$_{0.22}$ [a]	0.22	7.7
4	L-leu/HT$_{\text{rus}}$-A$_{0.44}$ [a]	0.44	7.8
5	L-leu/HT$_{\text{rus}}$-B$_{1.09}$ [b]	1.09	19.3

[a] Standard synthesis conditions of L-leu/HT$_{\text{rus}}$-A$_x$: L-leu (64, 256 and 768 mg), HT$_{\text{rus}}$ (500 mg), water (40 ml). T: 25 °C, 30 min.

[b] Standard synthesis conditions of L-leu/HT$_{\text{rus}}$-B$_x$: L-leu (980 mg), HT$_{\text{rus}}$ (500 mg), water (40 ml). T: 80 °C, 3 h.

[c] Determined by TOC.

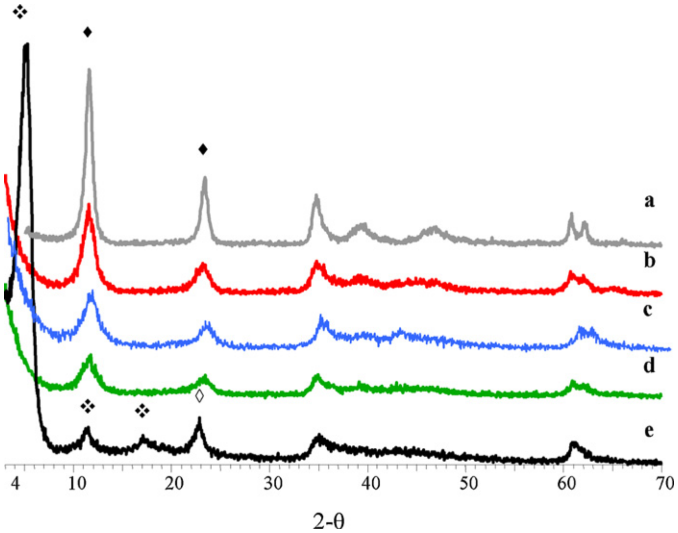

Fig. 1. XRD patterns of the nanohybrids synthesized by method A and B: (a) HT$_{\text{rus}}$, (b) L-leu/HT$_{\text{rus}}$-A$_{0.08}$, (c) L-leu/HT$_{\text{rus}}$-A$_{0.22}$, (d) L-leu/HT$_{\text{rus}}$-A$_{0.44}$, (e) L-leu/HT$_{\text{rus}}$-B$_{1.09}$. (♦) Basal peaks of (0 0 3) and (0 0 6) of HT$_{\text{rus}}$. (❖) Basal peaks of planes (0 0 3), (0 0 6) and (0 0 9) of the HT$_{\text{rus}}$ with L-leu intercalated. (◇) Basal peak of L-leu.

the stirring time. The L-leu of the two types of synthesized L-leu/HT$_{\text{rus}}$ nanohybrids (A and B) was believed to be immobilized mainly: (i) on the surface or at the edges sites of HT$_{\text{rus}}$ in the case of the L-leu/HT$_{\text{rus}}$-A$_x$ and (ii) by intercalation between the layers in the case of the L-leu/HT$_{\text{rus}}$-B$_x$. This was determined on the basis of characterisation by XRD, FTIR, HRTEM ^{13}C and ^{27}Al MAS NMR. The amount of L-leu anchored was determined by TOC analysis which measure total organic carbon of the ionized aqueous solution of L-leu (Table 1). Methodology A (immobilization process performed at r.t. and shorts times, 30 min) showed that the higher concentration of L-leu in the aqueous solution, the greater the amount of L-leu immobilized into the HT$_{\text{rus}}$. However, the maximum molar ratio L-leu/Al^{3+} immobilized was 0.44, (entry 4, Table 1).

The XRD analysis obtained for these catalysts presented a meixnerite structure (JCPDS 35-0965). The observed d_{003} basal spacing of the HT$_{\text{rus}}$ that appeared at 7.7 Å remained unchanged even after the anion exchange, which indicates that L-leu is mainly located at the edge positions or on the surface but not between the layers (entries 1–4, Table 1). The effect of the higher amount of L-leu immobilized in the HT$_{\text{rus}}$ is also observed in the XRD through the loss of the hydrotalcite crystallinity (Fig. 1a–d). A sharp signal in the ^{27}Al MAS NMR spectra at 9.0 ppm showed six-coordination with octahedral symmetry which indicated a non-very significant deformation of the HT$_{\text{rus}}$ layers after the immobilization of L-leu [29]. Therefore the lower crystallinity of the nanohybrids with higher content of L-leu is probably due to a greater amount of L-leu immobilized on the surface of the HT$_{\text{rus}}$.

A remarkable difference was observed in the nanohybrid synthesized by the methodology B (immobilization process performed at 80 °C for 3 h). The AA was added at a higher concentration than in the methodology A to favour the L-leu intercalation. The methodology B permitted a stoichiometric amount of L-leu immobilized in the HT$_{\text{rus}}$ (entry 5, Table 1). The XRD showed a d_{003} basal spacing at 19.3 Å indicating the intercalation of the L-leu between the HT$_{\text{rus}}$ layers (entry 5 Table 1 and Fig. 1e).

These results agree with the HRTEM images in Fig. 2. Fig. 2a corresponds to the sample L-leu/HT$_{\text{rus}}$-A$_{0.22}$ which showed platelet morphology indistinguishable from that of the starting HT$_{\text{rus}}$ material. Moreover, the basal lattice spacing calculated from FT analysis was 7.7 Å and it was well-defined throughout the entire nanohybrid material. This suggests that L-leu was not incorporated into the hydrotalcite layers. In contrast, the sample L-leu/HT$_{\text{rus}}$-B$_{1.09}$ exhibited a quite distinctive morphology (Fig. 2b). Platelets of the hydrotalcite structure are no longer well-preserved and they showed a low-order layer arrangement. This is accompanied by an increase of the basal lane lattice spacing, 19.5 Å.

The ionic state of AA can be estimated by FTIR and ^{13}C MAS NMR. Fig. 3 shows the FTIR spectra of the nanohybrid materials synthesized by method A and B. In the samples L-leu/HT$_{\text{rus}}$-A$_{0.44}$ and L-leu/HT$_{\text{rus}}$-B$_{1.09}$ spectra (Fig. 3b and c), a number of sharp components can be assigned to the aminoacid molecules besides the vibrational bands typical of the inorganic matrix. As for the sample L-leu/HT$_{\text{rus}}$-B$_{1.09}$, there are no significant differences in the OH stretching region (3700–3200 cm^{-1}) of the spectrum for the pure HT$_{\text{rus}}$ and the L-leu/HT nanohybrid materials. Fudala et al. also observed this effect for the L-phenilalanine–Zn–Al hydrotalcite compound and has been ascribed by these authors to the deprotonated form of the aminoacid taking part in the immobilization process [30]. On the other side, the broadening of the OH stretching bands in the spectrum of sample L-leu/HT$_{\text{rus}}$-A$_{0.44}$ points out that in this case some interaction between the organic molecule and HT hydroxy groups occurs (Fig. 3c).

In the L-leu/HT$_{\text{rus}}$-B$_{1.09}$ spectra (Fig. 3b), bands due to C–H stretching mode appear at 2900 cm^{-1} (νCH) and 2870 cm^{-1} (νCH_3). The broad component at 3064 cm^{-1} is assigned to NH_3^+ stretching mode. Accordingly, multiple peaks in the range of 2800–2400 cm^{-1} are assigned to combination bands and Fermi resonance involving NH_3^+ deformation modes, while the band at 2130 cm^{-1} is due to a combination band of asymmetric deformation and hindered rotation modes of the NH_3^+ group [31]. The presence of several weak and sharp bands at 1134, 1174 and 1188 cm^{-1} is also consistent with the presence of NH_3^+ group in the ionic form of the aminoacid [32]. All this bands associated with NH_3^+ group, clearly detected in the L-leu/HT$_{\text{rus}}$-B$_{1.09}$ sample spectra, are not observed in the spectrum of sample L-leu/HT$_{\text{rus}}$-A$_{0.44}$ (Fig. 3c). We do not exclude that it could be due to very low band intensities which do not allow the investigation of weak infrared components.

In the lower frequency region, the L-leu spectrum also presents strong absorption bands at 1576 cm^{-1} and 1405 cm^{-1}, assigned to the anti-symmetric and symmetric COO vibration stretching mode of the pure aminoacid carboxylate group (Fig. 3a). On the other side, the bands detected in the spectra of the both types of nanohybrid synthesized (A and B) at 1583 and 1582 cm^{-1} and 1406 and 1407 cm^{-1}, respectively, correspond to the asymmetric and symmetric stretching of the carboxilate group present in the ionic aminoacid form, shifted by the interaction with the inorganic matrix. Moreover, the broadening of the carboxylate bands in the L-leu/HT$_{\text{rus}}$-A$_{0.44}$ sample spectrum, should point out the formation of different types of carboxylates, whose coordination state changes in the hybrid form.

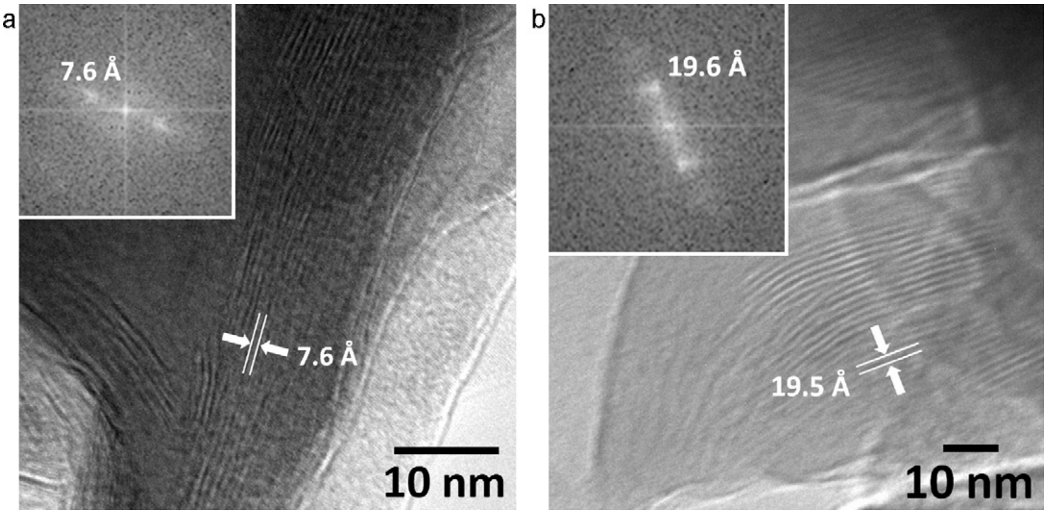

Fig. 2. HRTEM images of the nanohybrids synthesized by method A and B: (a) L-leu/HT_{rus}-$A_{0.22}$, (b) L-leu/HT_{rus}-$B_{1.09}$.

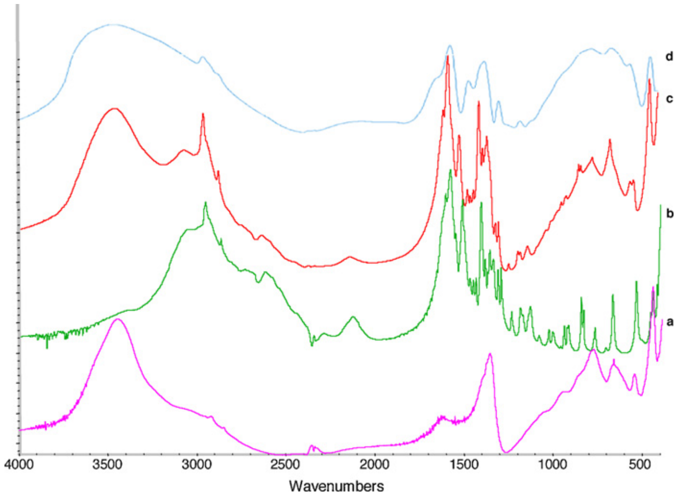

Fig. 3. FTIR skeletal spectra of nanohybrid by method A and B: (a) HT_{rus}, (b) L-leu, (c) L-leu/HT_{rus}-$B_{1.09}$ and (d) L-leu/HT_{rus}-$A_{0.44}$.

The ^{13}C chemical shift value of C=O carbon is very sensitive to ionic state of the AA [33]. Table 2 shows the chemical shift values of L-leu/HT_{rus}-$A_{0.44}$ and L-leu/HT_{rus}-$B_{1.09}$ (entries 3 and 4) together with those of L-leu$^-$ in aqueous basic solution (entry 1) and L-leu as a solid (entry 2). The chemical shift values of nanohybrids solids (entries 3 and 4) were similar to the L-leu$^-$ values (entry 1) showing a band at 185 ppm which confirms the presence of the carboxylate group.

Characterization of L-leu/HT_{rus}-A_x and L-leu/HT_{rus}-$B_{1.09}$ compounds shows that it is possible to obtain different kind of nanohybrid materials by variation in temperature and time of synthesis. The aminoacids in the L-leu/HT-A_x materials were immobilized in the edge and on the surface of the rehydrated hydrotalcite through a quick acid–base reaction between the hydroxyl groups of the HTs and the carboxilate group of L-leu. In the L-leu/HT-$B_{1.09}$ synthesis, both time and temperature were increased and the immobilization process occurred by ionic exchange of the L-leu and the hydroxyl groups in the interlayer space as it was indicated in the XRD and HRTEM analyses.

Table 2
^{13}C MAS NMR characterization of the L-leu/HT_{rus} nanohybrids.

Entry	Nanohybrid	COO(H)	C_α δ (ppm)	C_β	C_γ δ	C_δ δ
1[a]	L-leu$^-$	185	57	46	27	24
2[b]	L-leu	176	55	44	27	24
3[b]	L-leu/HT_{rus}-$A_{0.44}$	185	58	47	27	24
4[b]	L-leu/HT_{rus}-$B_{1.09}$	185	59	46	26	24

[a] L-leu in aqueous basic solution determined by ^{13}C NMR [14].
[b] Determined by ^{13}C MAS NMR.

Table 3
L-leu/HT_{rus}-catalayzed epoxidation of chalcone.[a]

Entry	Catalyst	Conv. (%)[b]	ee (%)[c]
0	–	<1	–
1	L-leu	9	–
2[d]	HT_{rus}	6	–
3[e]	L-leu/HT_{rus}-$A_{0.22}$	5	–
4[d]	L-leu/HT_{rus}-$A_{0.22}$	7	–
5	L-leu/HT_{rus}-$A_{0.08}$	18	0.5
6	L-leu/HT_{rus}-$A_{0.22}$	41	0.5
7	L-leu/HT_{rus}-$A_{0.44}$	85	0.6
8	L-leu/HT_{rus}-$B_{1.09}$	16	12

[a] Standard conditions: 1.44 mmol chalcone, 1.5 equiv. NaOH 5 M, 1.5 equiv. H_2O_2 (30 wt.%). Solvent: 3 ml hexane. Co-catalyst: 0.042 mmol TBAB. Corresponding quantity of catalyst with an L-leu content of 58 mg. T: 25 °C. Time: 90 min. Total diastereoselectivity towards the *trans*-1,2-epoxi-1,3-diphenyl-propane-1-ona.
[b] Determined by ^{1}H NMR.
[c] Determined by chiral HPLC. Enantiomer excess of (R,S)-trans isomer.
[d] In the absence of NaOH.
[e] In the absence of TBAB.

3.2. *Catalytic results*

Conventional Julià–Colonna asymmetric epoxidation of α,β-unsaturated ketones is catalyzed by the poly-L-leu (PLL). Kelly et al. suggest that the catalysis is due to binding of the hydroperoxide enolate intermediate by the three N-terminal amidic N–H groups of poly-L-leu [34]. In our best knowledge, there are no examples of the asymmetric epoxidation reaction of α,β-unsaturated ketones such as chalcone using alone L-leu as catalyst. However, the synergic effect between the aminoacids immobilized and the hydrotalcite could be key to produce successful results in the epoxidation of chalcona. In this context, a typical asymmetric Julià–Colonna epoxidation reaction of chalcone was performed using the different nanohybrid materials such as hetereogeneized catalysts. The results are summarized in Table 3.

To find the optimal reaction conditions was carried out on a series of experiments. We studied the necessity of a phase transfer co-catalyst (PTC) as well as the effect of the basic properties of the hydrotalcite support in the epoxidation reaction of chalcone (entries 3 and 4, Table 3).

Geller et al. observed that the addition of a PTC improved reaction rates up to 30 min using poly-L-leucine-1,3-diaminopropane as catalyst without any separate pre-activation [35]. In the heterogeneized reaction using the nanohybrid catalyst L-leu/HT_{rus}-$A_{0.22}$ the presence of a phase transfer co-catalyst such as tetrabutylammonium bromide (TBAB) also improved notably the conversion from 5% to 41% of the *trans*-1,2-epoxy-1,3-diphenyl-propan-1-one (entry 3, Table 3). Moreover, the asymmetric Julià–Colonna epoxidation reaction needs a base such as NaOH to activate the hydrogen peroxide generating the hydroperoxide anion (^{-}OOH). The HT_{rus} contains stronger and more accessible ^{-}OH interlayer anions as active basic sites [20]. After the immobilization process, the nanohybrid could keep some of the HT_{rus} basic sites and activate the hydrogen peroxide instead of the sodium hydroxide. However, the low conversion obtained shows that the basic sites of the nanohybrid materials seem to be not enough or not accessible at all (entry 4, Table 3). Therefore, the catalysts were tested in the Julià–Colonna epoxidation reaction of chalcone using TBAB and a 5 M NaOH solution. In the proposed reaction conditions, the pure L-leu showed a very low activity toward the *trans*-1,2-epoxy-1,3-diphenyl-propan-1-one and the enantioinduction was nil (entry 1, Table 3). The basic catalyst Mg/Al 2:1 HT_{rus} was also tested presenting a very poor activity (entry 2, Table 3). The low activity of the HT_{rus} contrasts with the total goal conversions obtained by Kaneda et al. in the epoxidation reaction of chalcone [36]. They used the $Mg_{10}Al_2(OH)_{24}CO_3$ compound as catalyst and obtained a 99% conversion. Kaneda proposed that the hydroxyls of the hydrotalcite layers play an important role in the catalytic activity of the process. However, α,β-ketone isophorone epoxidation also worked using as catalyst Na_2CO_3 (53% conv.). These data suggest that the interlayer carbonate anions of the HTs also contribute significantly in the epoxidation reaction. In addition, the low Mg/Al molar ratio of hydrotalcite affected the catalytic activity negatively. A notable difference was observed in the epoxidation of chalcone with the nanohybrid catalysts L-leu/HT_{rus}-A_x (entries 5–7, Table 3). The catalyst L-leu/HT_{rus}-$A_{0.22}$ presented moderated conversion, 18%, which was improved to 85% using the nanohybrid catalyst with a higher L-leu/Al^{3+} molar ratio, L-leu/HT_{rus}-$A_{0.44}$. These results are explained by the formation of the complexes L-leu:chalcone and L-leu:HOO^{-} in neighbouring positions on the HT_{rus}. This fact facilitates the nucleophilic attack by the hydroperoxide ion on the chalcone double bond to generate the peroxy-enolate [37]. However, the L-leu immobilized on the external part of the support did not allow the chiral induction. On the other hand, the L-leu/HT_{rus}-$B_{1.09}$ catalyst, where L-leu is immobilized in the interlayer spacing of the HT_{rus}, presented enantioselectivity toward the product *trans*-(R,S)-epoxy-1,3-diphenyl-propan-1-one (12%). This is attributed to the synergic effect between the HT_{rus} and the AA, where AAs distributed in the more restricted space between the layers favour the chiral induction as the PLL. However, the conversion was moderate (16%) to lower accessibility of the chalcone molecules (entry 8, Table 3).

4. Conclusions

Different kind of biohybrid materials based on L-leu into a hydrotalcite rehydrated under ultrasounds (HT_{rus}) has been synthesized using two different methodologies based on the reconstruction method. The performed methodologies required shorter times of synthesis than the previous published. In addition, they allowed control of the location of the L-leu immobilized into the hydrotalcite; either by intercalation or by replacement of the OH-anions at the edge-interlayers sites of the meixnerite which generated biocatalysts with different properties. The synergistic effect between the organo-guest and the inorganic-host of the nanohybrids was clearly reflected in the activity and enantioselectivity of the Julià–Colonna epoxidation reaction. The results showed that the L-leu immobilized in the HT_{rus} is efficient in asymmetric epoxidation of chalcone and it depends on the L-leu location. The novel nanohybrids synthesized with L-leu on the external part of the support showed high conversion but non chiral induction. While the nanohybrid catalysts with the L-leu in the interlayer space of hydrotalcite permitted to obtain slightly enantio-enriched product.

Acknowledgements

The authors would like to thank the Ministerio de Ciencia e Innovación from Spain (CTQ2009-12520-) and to Rovira i Virgili University (2009AIRE-10) for the economical support. R.-A.M. expresses his thanks to Rovira i Virgili University for his predoctoral fellowship. F.M. and J. Ll. thanks to Generalitat de Catalunya for the ICREA ACADEMIA award.

References

[1] S.P. Newman, W. Jones, New J. Chem. (1998) 105.
[2] S. Vijaikumar, A. Dhakshinamoorthy, K. Pitchumani, Appl. Catal. A 340 (2008) 25.
[3] A.I. Khan, D. OǐHare, J. Mater. Chem. 12 (2002) 3191.
[4] G. Lagaly, K. Beneke, Colloid Polym. Sci. 269 (1991) 1198.
[5] K.G. Theng, The Chemistry of Clay-Organic Reactions, Wiley, New York, 1974.
[6] G.A. Ozin, Adv. Mater. 4 (1992) 612.
[7] Y. Lvov, K. Ariga, I. Ichinose, T. Kunitake, J. Am. Chem. Soc. 117 (1995) 6117.
[8] U. Constantino, M. Casciola, G. Pani, D.M. Jones, J. Rozière, J. Solid State Ionics 97 (1997) 261.
[9] J.-H. Choy, S.-Y. Kwak, J.-S. Park, Y.-J. Jeong, J. Portier, J. Am. Chem. Soc. 121 (1999) 1399.
[10] J.-H. Choy, S.-Y. Kwak, J.-S. Park, Y.-J. Jeong, Angew. Chem. Int. Ed. 39 (2000) 4042.
[11] S. Aisawa, Y. Ohnuma, K. Hirose, S. Takahashi, H. Hirahara, E. Narita, Appl. Clay Sci. 28 (2005) 137.
[12] M. Darder, M. López-Blanco, P. Aranda, F. Leroux, E. Ruiz-Hitzky, Chem. Mater. 17 (2005) 1969.
[13] S. Aisawa, N. Higashiyama, S. Takahashi, H. Hirahara, D. Ikematsu, H. Kondo, H. Nakayama, E. Narita, Appl. Clay Sci. 35 (2007) 146.
[14] H. Nakayama, N. Wada, M. Tsuhako, Int. J. Pharm. 269 (2004) 469.
[15] B.M. Choudary, B. Kavita, N. Sreenivasa, B. Sreedhar, M. Lakshmi, Catal. Lett. 78 (2001) 1.
[16] F. Li, X. Duan, Struct. Bond 119 (2006) 193.
[17] X. Duan, D.G. Evans, Layered Double Hydroxides, Springer, Germany, 2006.
[18] V.R.L. Constantino, T.J. Pinnavaia, Inorg. Chem. 34 (1995) 883.
[19] T. Hibino, Chem. Mater. 16 (2004) 5482.
[20] R.J. Chimentaő, S. Abelló, F. Medina, J. Llorca, J.E. Sueiras, Y. Cesteros, P. Salagre, J. Catal. 252 (2007) 249.
[21] B.M. Adger, J.V. Barkley, S. Bergeron, M.W. Cappi, B.E. Flowerdew, M.P. Jackson, R. McCague, T.C. Nugent, S.M. Roberts, J. Chem. Soc. Perkin Trans. 1 (1997) 3501.
[22] M.W. Cappi, W.-P. Chen, R.W. Flood, Y.-W. Liao, S.M. Roberts, J. Skidmore, J.A. Smith, N.M. Williamson, Chem. Commun. 10 (1998) 1159.
[23] P. Verdié, G. Subra, P. Chevallet, M. Amblard, J. Martinez, Int. J. Pept. Ther. 13 (2007) 337.
[24] L. Carde, D.H. Davies, S.M. Roberts, J. Chem. Soc. Perkin Trans. 1 (2000) 2455.
[25] S. Juliá, S. Colonna, J. Chem. Soc. Perkin Trans. 1 (1982) 1317.
[26] G. Carrea, S. Colonna, D. Kelly, A. Lazcano, G. Ottolina, S. Roberts, Trends Biotechnol. 23 (2005) 507.
[27] A. Berklessey, N. Gasch, K. Glaubitz, C. Koch, Org. Lett. 3 (2001) 3839.
[28] S. Abelló, F. Medina, D. Tichit, J. Pérez-Ramírez, J.C. Groen, J.E. Sueiras, P. Salagre, Y. Cesteros, Chem. Eur. J. 11 (2005) 728.
[29] J. Rocha, M. Del Arco, V. Rives, M.A. Ulibarri, J. Mater. Chem. 9 (1999) 2499.
[30] A. Fudala, I. Palinkó, I. Kiricsi, Inorg. Chem. 38 (1999) 4653.
[31] N.B. Coulthup, L.H. Daly, S.E. Wiberley, Introduction to Infrared and Raman Spectroscopy, Academic Press, New York, 1964.
[32] P.F. Façanha Filho, P.-T.-C. Freire, K.C.V. Lima, J. Mendes Filho, F.E.A. Melo, Brazil. J. Phys. 38 (2008) 131.
[33] S. Tran-Dinh, S. Fermandjian, E. Sala, R. Memet-Bouvier, M. Cohen, P. Fromageot, J. Am. Chem. Soc. 96 (1974) 1484.
[34] D.R. Kelly, S.M. Roberts, Chem. Commun. (2004) 2018.
[35] T. Geller, A. Garlach, C.M. Krüger, H.-C. Militzer, J. Mol. Catal. A: Chem. 2251 (2006) 71.
[36] K. Yamaguchi, K. Mori, T. Mizugaki, K. Ebitani, K. Kaneda, J. Org. Chem. 65 (2000) 6897.
[37] D.R. Kelly, E. Caroff, R.W. Flood, W. Heal, S.M. Roberts, Chem. Commun. (2004) 2016.